



Platelet-Derived Biomaterials Inhibit Nicotine-Induced Intervertebral Disc Degeneration Through Regulating IGF-1/AKT/IRS-1 Signaling Axis

Wen-Cheng Lo^{1,2}, Chi-Sheng Chiou^{3,4}, Feng-Chou Tsai^{5,6},
Chun-Hao Chan^{3,7}, Samantha Mao⁷, Yue-Hua Deng^{3,7},
Chia-Yu Wu^{3,8}, Bou-Yue Peng^{3,8}, and Win-Ping Deng^{3,7,9,10} 

Cell Transplantation
Volume 30: 1–12
© The Author(s) 2021
Article reuse guidelines:
sagepub.com/journals-permissions
DOI: 10.1177/09636897211045319
journals.sagepub.com/home/ctt


Abstract

Apart from aging process, adult intervertebral disc (IVD) undergoes various degenerative processes. However, the nicotine has not been well identified as a contributing etiology. According to a few studies, nicotine ingestion through smoking, air or clothing may significantly accumulate in active as well as passive smokers. Since nicotine has been demonstrated to adversely impact various physiological processes, such as sympathetic nervous system, leading to impaired vasculature and cellular apoptosis, we aimed to investigate whether nicotine could induce IVD degeneration. In particular, we evaluated dose-dependent impact of nicotine in vitro to simulate its chronic accumulation, which was later treated by platelet-derived biomaterials (PDB). Further, during in vivo studies, mice were subcutaneously administered with nicotine to examine IVD-associated pathologic changes. The results revealed that nicotine could significantly reduce chondrocytes and chondrogenic indicators (Sox, Col II and aggrecan). Mice with nicotine treatment also exhibited malformed IVD structure with decreased Col II as well as proteoglycans, which was significantly increased after PDB administration for 4 weeks. Mechanistically, PDB significantly restored the levels of IGF-1 signaling proteins, particularly pIGF-1 R, pAKT, and IRS-1, modulating ECM synthesis by chondrocytes. Conclusively, the PDB impart reparative and tissue regenerative processes by inhibiting nicotine-initiated IVD degeneration, through regulating IGF-1/AKT/IRS-1 signaling axis.

Keywords

nicotine, Intervertebral disc degeneration, Platelet-derived biomaterials, IGF-1

Introduction

Intervertebral discs (IVDs) degeneration is well-known to contribute to back, neck as well as radicular pain in aging

population¹. During early degenerative events, a reduced cell population in the inner, gelatinous nucleus pulposus (NP) of IVD is the notable hallmark. NP cell is generally considered

¹ School of Medicine, College of Medicine, Taipei Medical University, Taipei

² Department of Neurosurgery, Taipei Medical University Hospital, Taipei

³ School of Dentistry, College of Oral Medicine, Taipei Medical University, Taipei

⁴ Division of Allergy, Immunology and Rheumatology, Department of Internal Medicine, Taipei Medical University Hospital, Taipei

⁵ Department of Surgery, School of Medicine, College of Medicine, Taipei Medical University, Taipei 110301

⁶ Division of Plastic Surgery, Department of Surgery, Shuang Ho Hospital, Taipei Medical University, New Taipei City

⁷ Stem Cell Research Center, College of Oral Medicine, Taipei Medical University, Taipei

⁸ Division of Oral and Maxillofacial Surgery, Department of Dentistry, Taipei Medical University Hospital, Taipei

⁹ Graduate Institute of Basic Medicine, Fu Jen Catholic University, New Taipei City

¹⁰ Department of Life Science, Tunghai University, Taichung

Submitted: July 25, 2021. Revised: August 20, 2021. Accepted: August 24, 2021.

Corresponding Author:

Win-Ping Deng, Taipei Medical University, Taipei 11031.

Email: wpdeng@tmu.edu.tw



Creative Commons Non Commercial CC BY-NC: This article is distributed under the terms of the Creative Commons Attribution-NonCommercial 4.0 License (<https://creativecommons.org/licenses/by-nc/4.0/>) which permits non-commercial use, reproduction and distribution of the work without further permission provided the original work is attributed as specified on the SAGE and Open Access pages (<https://us.sagepub.com/en-us/nam/open-access-at-sage>).

as chondrocyte-like cells^{2,3}, which its tissue is composed of proteoglycans (PGs), assisting the retention of water to withstand the compression, transfer and distribution of spinal loads between vertebral bodies while maintaining their mobility⁴. This pathologic condition has been attributed to elevated levels of pro-inflammatory cytokines such as TNF, and interleukins such as IL-1, IL-6, and IL-17 in IVD cells, promoting extracellular matrix degradation, chemokine production and changes in IVD phenotype. The several etiologic factors underlying IVD degeneration include mechanical damage, genetic variations and exposure to pathogenic substances⁵. Besides, many previous studies have revealed that smoking is highly correlated to back pain, and tobacco users may display IVD degenerative characteristics^{6,7}. Of tobacco products, nicotine is well-known to be a major addictive component which may contribute to various pathophysiologies including IVD degeneration^{8,9}, possibly through vasoconstriction, arteriosclerotic, carboxy-hemoglobin production, changes in blood flow, and impaired fibrinolytic activity¹⁰⁻¹². Besides, passive cigarette smoking has also been implicated in exerting histologic changes in intervertebral disc¹³, indicating that nicotine exposure may contribute to degeneration of IVD; however, the underlying mechanism still remain unclear. Therefore, in order to confirm nicotine-induced IVD pathology, we established mouse model of nicotine-induced IVD degeneration. Of note, since creating the animal models mimicking chronic accumulation of toxic chemicals like nicotine seems difficult to manifest its dose-dependent impact; hence, higher doses of nicotine were applied during in vitro studies. In addition to our previous study on nicotine-induced osteoarthritis¹⁴, another seminal study has already employed higher doses of nicotine on human umbilical vein endothelial cells (HUVECs) to mimic chronic accumulation of nicotine-induced toxicity, which revealed progression of periodontal disease as well as cardiovascular disease¹⁵.

Besides, the positive impact of traditional/current therapies for degenerative IVD is still very limited, and often resulted in inability to relieve the pain, or accelerated adjacent segment degeneration. Hence, restoring adequate functional behavior by maintain disc height and spine curvature in IVD remains a challenge. In recent years, cell-based biological therapies are gaining attention to provide a more biological approach, with minimal adverse effects. In the recent years, platelet-derived biomaterials (PDB), a whole blood-extracted biomaterial enriched with platelets and various growth factors, has been widely used as regenerative medicine. PDB contains several prominent growth factors including platelet-derived growth factor (PDGF), transforming growth factor- β (TGF- β), insulin-like growth factor-1 (IGF-1), epidermal growth factor (EGF), bone morphogenetic protein (BMP)-2 and BMP-7, which have also been implicated in our previous study to restore extracellular matrix (ECM) of cerebral, renal and knee-joint pathologies^{14,16}. Moreover, research had indicated the composition and degeneration process of articular joint and IVD are quite

similar¹⁷, which motivated us to further investigate whether nicotine and PDB exhibit the consistent effects on IVD. However, the pathophysiologies of IVD degeneration still differed from knee osteoarthritis. Knee joint osteoarthritis is characterized by loss of chondrocytes and narrowing of joint space¹⁸, whereas IVD degeneration responsible for back pain is associated with changes during disc which includes hypocellularity, low extracellular matrix (ECM) and reduced disc height¹⁹. Also, the avascular articular cartilage is nourished by both subchondral bone marrow and synovial²⁰, whereas in IVD tissue such as NP cells are rely on nutrients supplied from cartilaginous endplate route, while the cells in the annulus fibrosus region are mainly nurtured by annulus peripheral pathway²¹. Hence, we were interested whether PDB shares similar therapeutic mechanism in these two different pathophysiologies. Therefore, this study investigated the ameliorative effect of PDB therapy on nicotine-induced IVD degeneration, and further explored the underlying mechanism.

In our study, we established a chronic degenerative IVD in vitro model by treating immortalized human nucleus pulposus cells (ihNPs) with high-doses of nicotine, which was determined in the terms of chondrogenic gene and protein expressions. Later, PDB was then administered to nicotine-treated ihNPs for determining its therapeutic potential. Further, the effects of PDB was also evaluated in neo-cartilage model, which is a 3D collagen scaffold containing ihNPs, for mimicking the in vivo cartilage microenvironment. Finally, we developed in vivo nicotine-induced IVD degeneration mice model as pre-clinical study to investigate the therapeutic potential of PDB and explored the possible underlying mechanism.

Materials and Methods

Establishment of Immortalized Human Nucleus Pulposus cells (ihNPs) and Ethics

To establish the immortalized hNPs, hNPs were isolated from the healthy IVD of a 39 years old male donor. Informed consent was provided by the volunteer for using the NP cells in accordance with the principles of the Ethics Committee of Taipei Medical University Hospital, Taiwan. The NP tissue was collected aseptically and cut into pieces in the Hank's balanced salt solution (HBSS; Gibco BRL) containing antibiotics. Enzymatic solution (0.4% collagenase I and 0.04% protease, purchased from Sigma) was then treated for 4 h at 37°C to isolate NP cells. Later, the cell suspension was filtered by 40- μ m nylon mesh, centrifuged, then resuspended in the Dulbecco's modified Eagle's medium (DMEM/F-12; Gibco BRL) with 10% fetal bovine serum (FBS). The isolated NP cells were cultured in 10-cm dishes and maintained in 5% CO₂ incubator at 37°C prior to successive experiments. Later, as described in the previous study, the isolated hNPs were immortalized through transfecting them with retroviral vector-driven HPV16 E6/E7²². Briefly, the HPV-16

E6/E7 retroviral vector (LXSN16E6E7)^{22,23} carrying a virus produced from PA317 cell line (from the American Type Culture Collection (ATCC)) was expanded in DMEM containing 10% FBS (Gibco). The isolated primary hNPs were seeded on 6-well plates at a density of 2.5×10^5 cells/well, then infected with 1 mL of viral stock in medium containing 8 μ g/mL polybrene for 48 h. The virus removal was done by replacing with DMEM/F12 medium supplemented with 10% FBS. Cell passaging was done on the next day at 1:3 ratio. After 3 weeks of transduction, cells were harvested when obvious clones of actively dividing cells developed. Similar to primary cultures, the infected ihNPs were grown in the same medium twice a week and passaged at a 1:3 ratio when the cells appeared subconfluent.

PDB Preparations and Cell Proliferation

The preparation and quantification of PDB has been described in a previous study²⁴. Briefly, whole blood was procured from Taipei Blood Center and separated using MCS blood cell separation system (Haemonetics Corp., Braintree, MA). Thereafter, bovine thrombin was applied and centrifuged with 3000 rpm at room temperature for 6 minutes to remove the aggregated fibrin, then PDB was prepared and stored at -20°C . PDB concentrations were determined through TGF- β 1 by enzyme-linked immunosorbent assay. The 5×10^5 cells/ml ihNPs were seeded into six-well plate, and then PDB (TGF- β 1 = 1 ng/ml)-conditioned medium was later treated, while medium with 1% FBS was employed as experimental control. After 7 days of treatment, the effects of nicotine (Sigma 36733, USA) and PDB on cell proliferation and their numbers were determined using automated cell counter Countess™ (Life Technologies, Carlsbad, USA).

Real-Time Polymerase Chain Reaction (qPCR)

Total RNA was extracted using High Pure RNA Isolation Kit (Roche, Germany) in accordance with manufacturer's protocols. Reverse transcription-PCR (RT-PCR) was performed as described in the previous study²⁵. The qPCR assay was conducted using ABI 7300 real-time detection PCR system (Applied Biosystems, USA), and the relative gene expression was evaluated by $2^{-\Delta\text{Ct}}$ or $2^{-\Delta\Delta\text{Ct}}$ approach with calibration samples in each experiment. Primers utilized are listed below:

SOX9 – Forward: AGACCTTTGGGCTGCCTTAT;

Reverse: TAGCCTCCCTCACTCCAAGA

Col II – Forward: CCTTCCTGCGCCTGCTGTC;

Reverse: GGCCCGATCTCCACGTC

Aggrecan – Forward: CCGCTACGACGCCATCTG;

Reverse: CCCCCACTCCAAAGAAGTTTT

MMP-1 – Forward: AGCTAGCTCAGGATGACATTGATG;

Reverse: GCCGATGGGCTGGACAG

MMP-3 – Forward: TGGCATTACAGTCCCTCTATGG

Reverse: AGGACAAAGCAGGATCACAGTT

MMP-9 – Forward: CCTGGAGACCTGAGAACCAATC

Reverse: CCACCCGAGTGTAACCATAGC

β -actin – Forward: AGAGCTACGAGCTGCCTGAC

Reverse: AGCACTGTGTTGGCGTACAG

Western Blotting

Cell lysis was done in radioimmunoprecipitation assay buffer (RIPA buffer) (150 mM NaCl, 50 mM Tris, 1% NP-40, 0.5% deoxycholate (DOC), and 0.1% sodium dodecyl sulfate). The spinal discs were harvested from lumbar and tail segments through directly excision from vertebral body, then disc tissue was mixed with RIPA buffer and sonicated by Misonix XL-2000 ultrasonic liquid homogenizer (Misonix Inc., NY) for isolation of protein. Afterwards, the cellular total protein was isolated and denatured for 10 min at 100°C , then gel electrophoresis was performed to separate the proteins according to their different molecular weight. The separated proteins were later transferred to polyvinylidene difluoride (PVDF) membrane (Millipore, USA), and 4% bovine serum albumin (BSA) blocking buffer was done and incubated for 1 hour at room temperature to avoid non-specific binding. The membranes were further incubated with Sox9 (ab59252, 1:500, Abcam, Cambridge, UK), Col II (ab34712, 1:1000, Abcam), AGN (MABT83, 1:500, Millipore, Billerica, MA, USA), IGF-1 R (9750 S, 1:500, Cell Signaling, Danvers, MA, USA), pIGF-1 R (3024 S, 1:500, Cell Signaling), AKT (GTX121937, 1:2500, GeneTex, Irvine, CA, USA), pAKT (GTX59559, 1:1000, GeneTex), IRS-1 (GTX78916, 1:500, GeneTex), β -actin (GTX109639, 1:10000, GeneTex) and GAPDH (GTX100118, 1:10000, GeneTex) antibodies. Anti-rabbit secondary peroxidase-conjugated antibody (111-035-003; Jackson ImmunoResearch, Newmarket, UK) and anti-mouse secondary peroxidase-conjugated antibody (115-035-003, Jackson ImmunoResearch) were later applied and incubated for 1 hour at room temperature. The expression of protein bands were visualized through chemiluminescence detection kit (WBKLS0500, Millipore, USA) and the images were captured by Mutigel-21 (Fluorescent Gel Image System, Top-Bio, Taipei, Taiwan).

Formation of In Vitro 3D Neo-Cartilage and Histological Analysis

The protocol for ihNP neo-cartilage synthesis has already been previously described²⁶. Briefly, neo-cartilages were incubated in rotatory cell culture system (RCCS-4D[®], Synthcon, Houston, TX, USA) with DMEM/F12 (control group), nicotine (1,000 μ M) (disease group) and nicotine+PDB

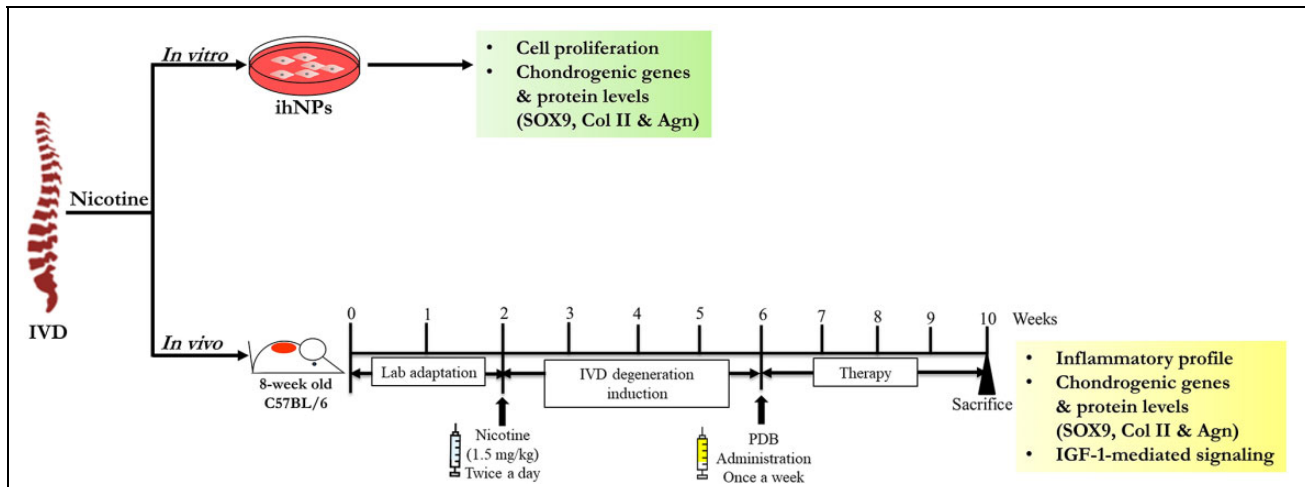


Figure 1. Schematic representing determination of nicotine impact on IVD in vitro as well as in vivo. ihNPs: Immortalized human nucleus pulposus cells, IVD: intervertebral disc.

(treatment group) containing medium respectively in a 5% CO₂ incubator at 37°C, and medium were replaced every 2 days. After 4-week culture period, neo-cartilages were sectioned for histological analysis. Hematoxylin and eosin (H&E) staining was further conducted for identifying ultra-structural changes, and immunohistochemical (IHC) staining of Col II (Millipore, Temecula, CA, USA) and alcian blue stain were performed to determine the accumulation of chondrogenic extracellular matrix (ECM) and proteoglycans, respectively.

Nicotine-Induced IVD Degeneration Animal Model

Eight-week-old male C57BL/6 mice ($n = 5$) were subcutaneously injected with 1.5 mg/kg nicotine to induced with IVD degeneration as per the previous study²⁷, while mice without any treatment were assigned as control ($n = 5$). After 1 month of nicotine administration, 100 μ l of PDB (1 ng/ml) was subcutaneously injected to the skin above the spine ($n = 5$) once per week for total 4 weeks. Thereafter, the animals were euthanized and the IVDs of each group were then harvested for histological and immunohistological studies.

Histological and Immunohistological Analysis

IHC staining of fixed tissue sections was performed via avidin-biotin peroxidase detection technique. In brief, the paraffin wax of the unstained section was removed by xylene and the tissue sections were then rehydrated using decreasing concentrations of ethanol. 4% BSA buffer was used to block non-specific binding. Further, avidin and biotin binding sites were blocked using a commercial avidin–biotin blocking kit (Vector Laboratories, USA). Tissue sections were firstly incubated with their respective antibodies for 30 minutes at room temperature, following by overnight incubation at 4°C. These sections were then rinsed in ice-

cold saline and incubated with secondary biotinylated anti-mouse immunoglobulin G. The 0.3% H₂O₂ in horseradish peroxidase (Vector Laboratories) was used to blocked the endogenous peroxidase activity, and the peroxidase activity was visualized by diaminobenzidine (Vector Laboratories). Slides were further rinsed in water and afterwards counterstained by hematoxylin. Additionally, the sections were further stained with Col II and alcian blue to observe the expression of cartilage and PG, respectively. The quantifications were performed using Image J software. Disc height index (DHI) was assessed from lumbar segment using method as described previously²⁸.

Statistical Analysis

Data are presented as mean \pm SD. The experiments were performed in at least three biological replicates if no further stated, and the statistical analysis was done with Student's *t*-test and one-way ANOVA with post-hoc Tukey HSD test (Sigma Plot Version 10.0 and GraphPad Prism 7). *P*-value <0.05 was considered statistically significant. The symbols *, **, and *** specify $P < 0.05$, $P < 0.01$, and $P < 0.001$, respectively.

Results

In order to assess the regenerative bioactivities impact of PDB against IVD degeneration, we established in vitro as well as in vivo animal models, the experimental schematic of which has been illustrated in Fig 1.

Nicotine Degenerated Immortalized Human Nucleus Pulposus Cells (ihNPs)

To ascertain the impact of chronic accumulation of nicotine on IVD degeneration, we administered higher dosage of nicotine on ihNPs. In particular, the proliferative characteristics of

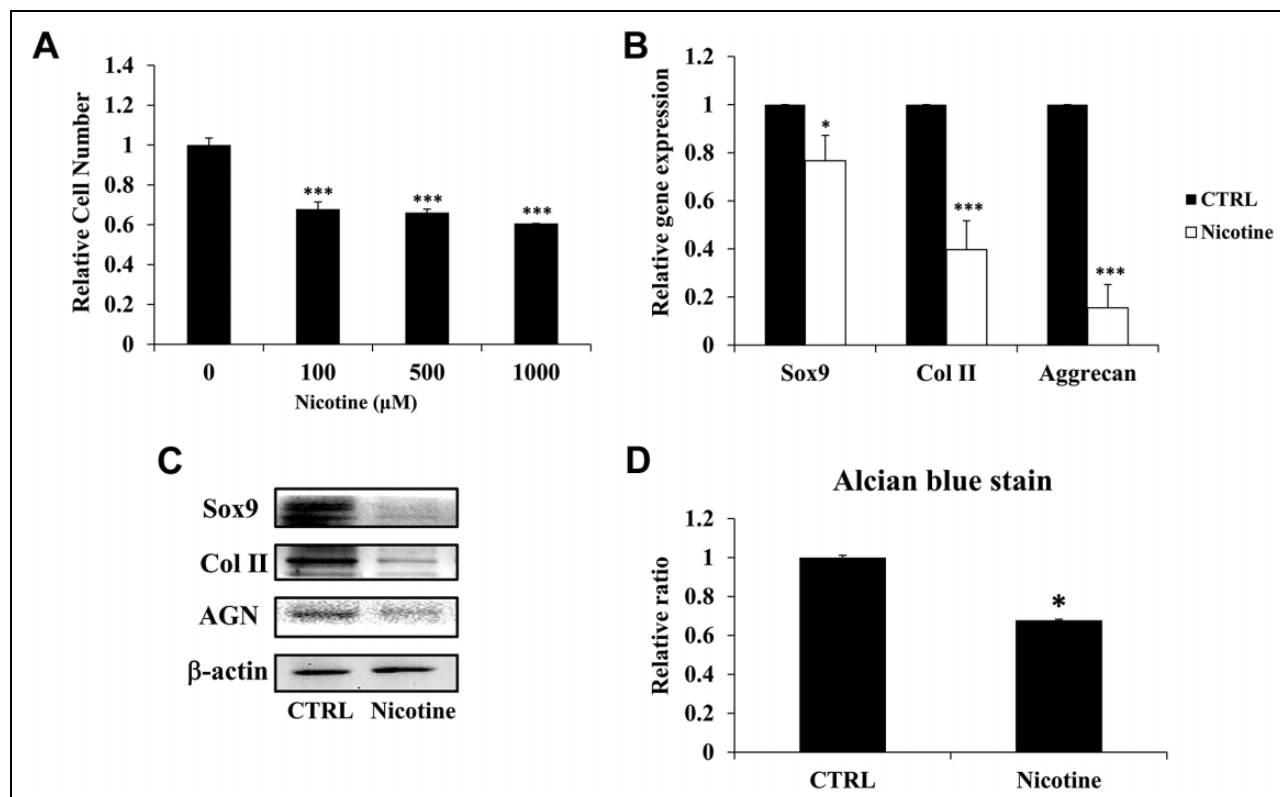


Figure 2. Impact of nicotine on ihNPs cellular activity and chondrogenic markers. Initially, immortalized human nucleus pulposus cells (ihNPs) of IVD were treated with 100 μ M, 500 μ M and 1000 μ M of nicotine for 7 days to evaluate its effects on proliferation ability (A). Owing to the increased deteriorating effect, concentration of 1000 μ M nicotine was applied for the further experiments. (B) Gene and (C) protein expressions of chondrogenic markers including Sox9, Col II, and aggrecan. We further relatively quantified the expression of alcian blue in control and nicotine-treated ihNPs (D). The results are presented as mean \pm S.D. ($n = 3$; * $P < 0.05$ and *** $P < 0.001$, respectively compared to control group).

ihNPs was determined through treating various concentration of nicotine (100 μ M, 500 μ M, and 1,000 μ M) for 7 days. In contrast to control group, all the nicotine-treated groups exhibited significantly declined cell numbers, particularly in 1000 μ M group (Fig. 2A). Hence, in the line with our previous report¹⁴, we employed 1000 μ M of nicotine in subsequent experiments to mimic chronic accumulation. We further investigated the degenerative effects of nicotine in ihNPs through examining cartilage-specific biomarkers (SOX9, Col II, Aggrecan), the results revealed that gene (Fig. 2B) and protein (Fig. 2C) levels of which were significantly suppressed after nicotine treatment. These results were further reinforced by the suppressed quantification levels of alcian blue staining in nicotine-treated group (Fig. 2D), indicating the loss of proteoglycans (PGs), which is a hallmark of IVD degeneration²⁹.

Chondroprotective and Chondroregenerative Impacts of Platelet-Derived Biomaterials (PDB) in Nicotine-Treated ihNPs

After confirming the deteriorating outcomes of nicotine on ihNPs, we evaluated whether PDB possess therapeutic

potential against it. Our results demonstrated that the reduced cell number of nicotine-treated ihNPs, was restored by PDB treatment (Fig. 3A). Meanwhile, the expressions of cartilage-specific proteins including SOX9, Col II and aggrecan were also enhanced at gene (Fig. 3B) as well as protein levels (Fig. 3C). These results indicate the chondroprotective and chondroregenerative characteristics of PDB which was further substantiated through alcian blue staining (Fig. 3D).

PDB Prevents Chondral Degeneration in 3D Neo-Cartilage Model

To simulate an in vivo environment, we further examined effects of PDB in a nicotine-treated 3D neo-cartilage model. After the treatment of PDB, the 3D neo-cartilage tissues were then sectioned for conducting H&E staining, IHC of type II collagen (Col II) and alcian blue staining. The H&E staining revealed a deformed morphology with decreased blue-purple color in nicotine-treated group (Fig. 4A-b) compared to control (Fig. 4A-a), which implied the reduction of nucleic acids in ihNPs; however, this reduction was restored by PDB treatment (Fig. 4A-c). Similarly, suppressed IHC

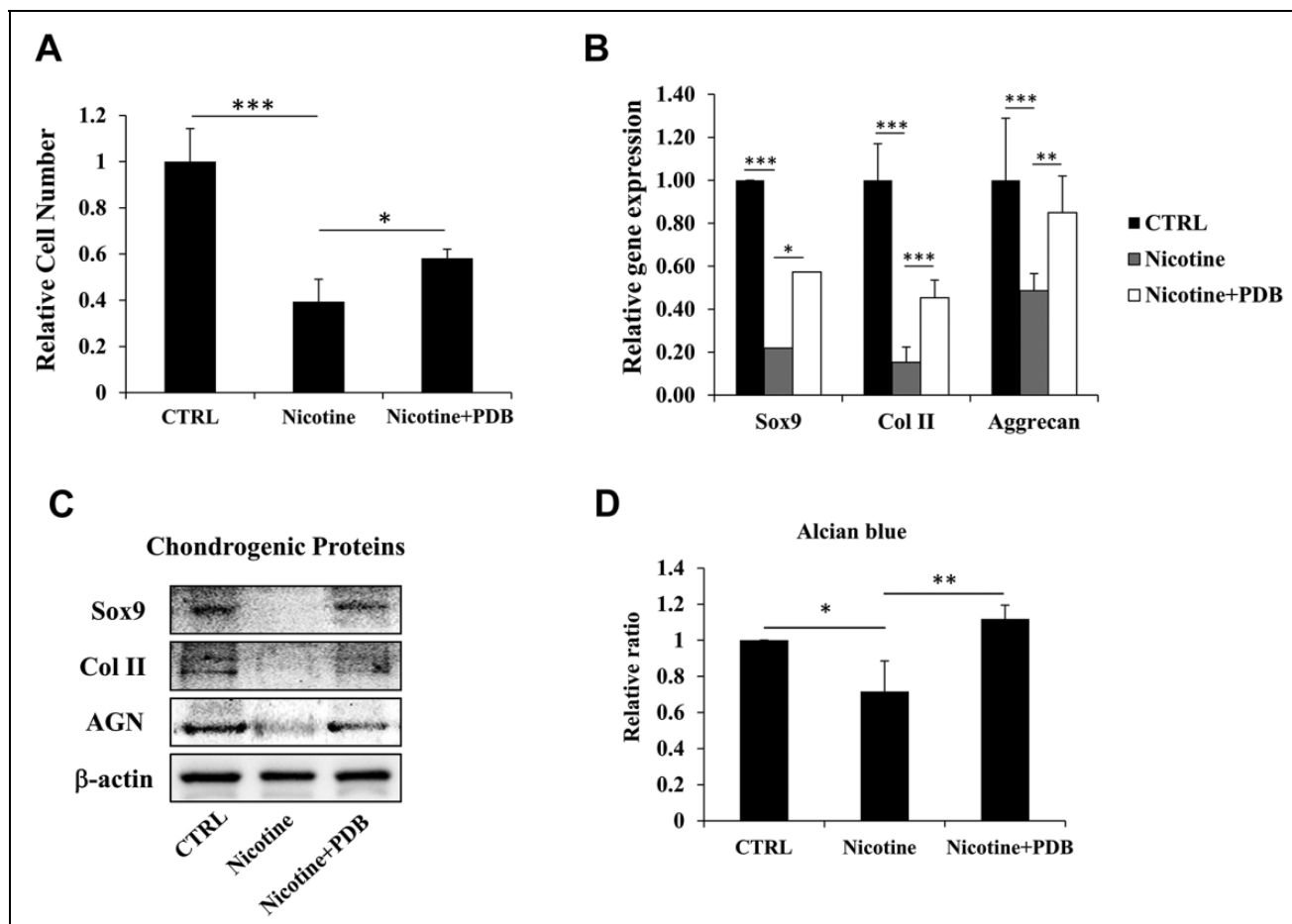


Figure 3. Therapeutic effects of platelet-derived biomaterials (PDB) on cell proliferation and chondrogenic markers of nicotine-treated ihNPs. Following PDB treatment for seven days, we investigated the (A) proliferation ability, (B) gene and (C) protein levels of chondrogenic markers including Sox9, Col II and aggrecan in ihNPs. (D) Quantification of alcian blue in control, nicotine-treated and PDB-treated ihNPs. Results are presented as mean \pm S.D. ($n = 3$; * $P < 0.05$, ** $P < 0.01$, *** $P < 0.001$).

Col II and alcian blue staining in nicotine-treated group implied reduced content of Col II and PGs (Fig. 4A, e and h), as compared to their respective controls (Fig. 4A, d and g). In contrast, Col II was significantly promoted while alcian blue signals showing increasing trend in PDB treatment group, indicated the restorative potential of PDB treatment (Fig. 4A, f and i). These data were further confirmed through their quantification (Fig. 4B, C, respectively).

PDB Prevents Nicotine-Induced IVD Degeneration *in Vivo*

Finally, to evaluate the *in vivo* remedial effects of PDB, C57BL/6 mice were subcutaneously injected with nicotine (1.5 mg/kg/day) for 4 weeks to induce IVD degeneration. Thereafter, PDB was subcutaneously applied to the mice for further 4 weeks. After PDB treatment, spinal tissues were sectioned and staining were subsequently conducted to observe the physiological effects of nicotine and PDB to the IVD. The H&E staining revealed that compared to control

(Fig. 5A-a), a narrowed and flattened morphology of nucleus pulposus and intervertebral space were exhibited in nicotine-treated group (Fig. 5A-b), which was recovered by PDB treatment (Fig. 5A-c). Further, the reduction of Col II and alcian blue signals in the nicotine-treatment groups (Fig. 5A, e and h) were observed when compared to their respective controls (Fig. 5A, d and g), which was restored through PDB administration (Fig. 5A, f and i). The Col II and alcian blue signals were further validated through their respective quantification (Fig. 5B, C, respectively). Additionally, the disc height index was further measured in the H&E staining sections (Fig. 5D), in which the results showing PDB recovered the DHI, which was decreased by nicotine (Fig. 5E).

PDB Regulated Signaling Pathways in Nicotine-Induced IVD Degeneration

To investigate the underlying signaling pathway of PDB-inhibited IVD degeneration, the isolated RNA and protein from IVD tissue were further employed. Previous research

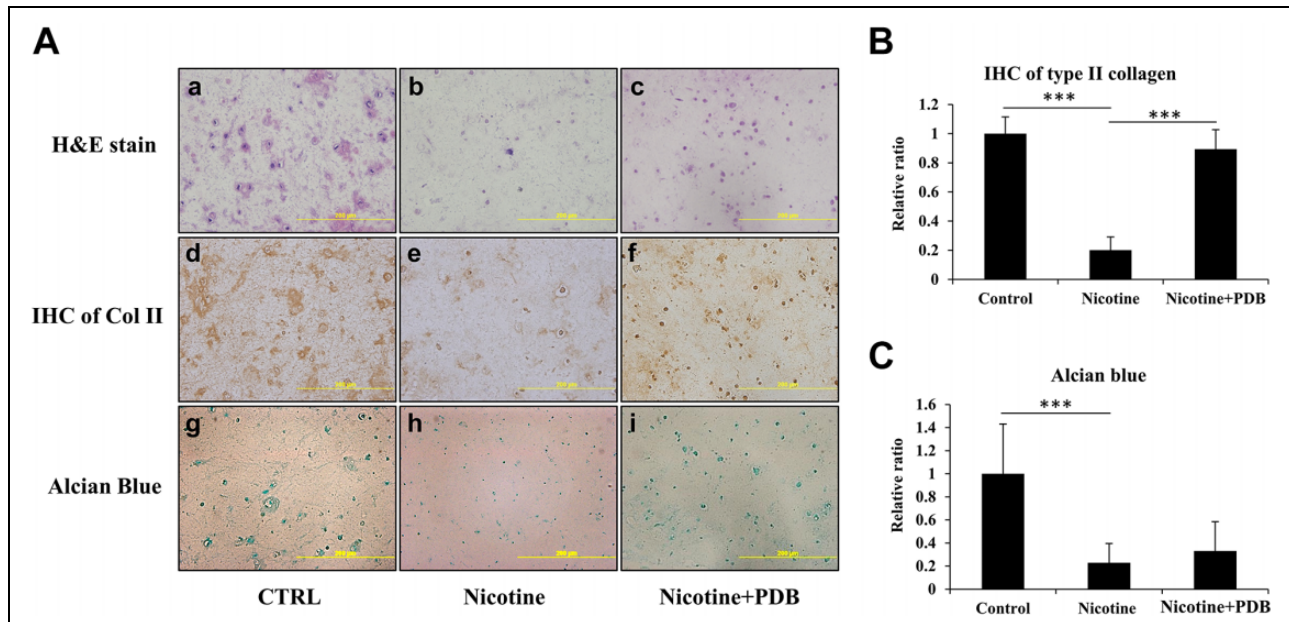


Figure 4. Chondral regeneration effects of PDB on nicotine-treated 3D neo-cartilage IVD model. We conducted (A) Hematoxylin & eosin (H&E) staining (a-c, upper panel), immunohistochemistry staining of Col II (IHC Col II) (d-f, middle panel) and alcian blue staining (g-i, lower panel) to ascertain the morphologic alterations, collagen and proteoglycan expressions, respectively in control, nicotine-treated and PDB-treated nicotine-IVD group. All the images were captured at 20X magnification (Scale bar: 200 μ m). Additionally, these staining signals of (B) Col II and (C) alcian blue were relatively quantified. The results are presented as mean \pm S.D. ($n = 3$; *** $P < 0.001$).

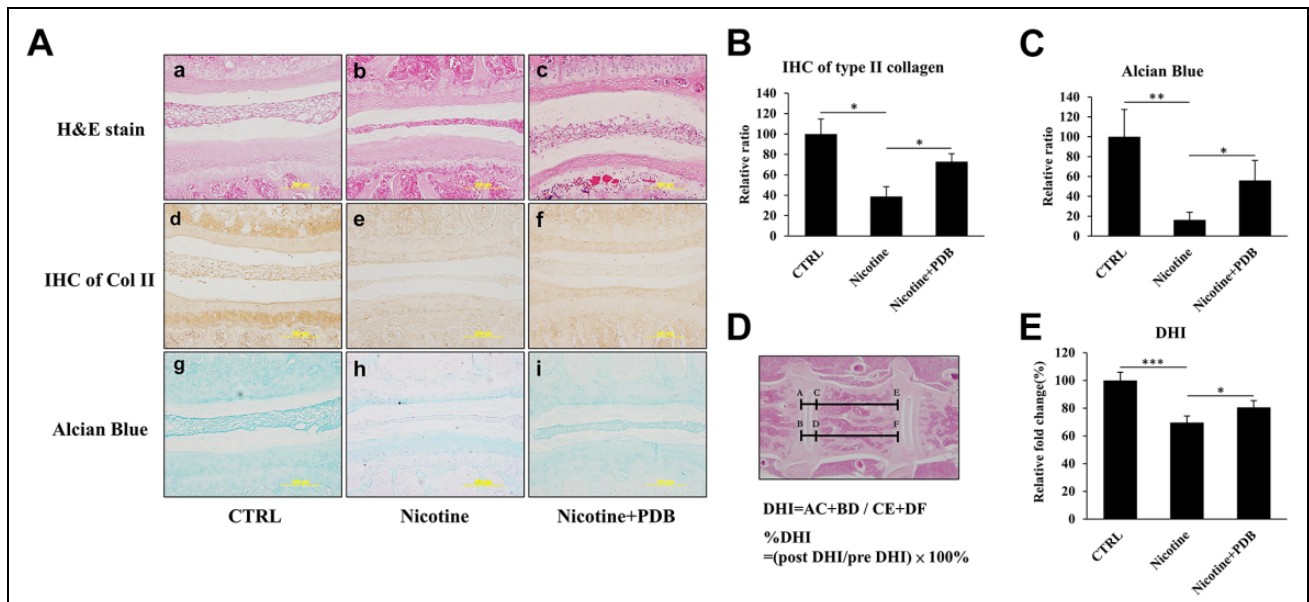


Figure 5. PDB and in vivo IVD-associated histologic improvements. After 2 weeks of lab adaptation, mice ($n = 5$) were subcutaneously injected with nicotine (1.5 mg/Kg/day) for 4 weeks. Thereafter, animals ($n = 5$) were subcutaneously administered with PDB once per week for next 4 weeks, and progressive improvement in IVD was assessed. We specifically determined ultrastructural alterations, collagen and proteoglycan content, respectively by (A) Representative hematoxylin & eosin (H&E) staining (a-c, upper panel), immunohistochemical staining of Col II (IHC Col II) (d-f, middle panel) and alcian blue staining (g-i, lower panel) in control, nicotine-treated and PDB-treated nicotine-IVD groups. All the images were captured at 20X magnification (Scale bar: 200 μ m). The quantification of Col II and alcian blue signals were also shown in (B) and (C), respectively. (D) Measurement and calculation of DHI values based on the H&E staining sections, which were further presented as their relative fold change (E). The results are presented as mean \pm S.D. ($n = 5$; * $P < 0.05$, *** $P < 0.001$). DHI: Disc height index.

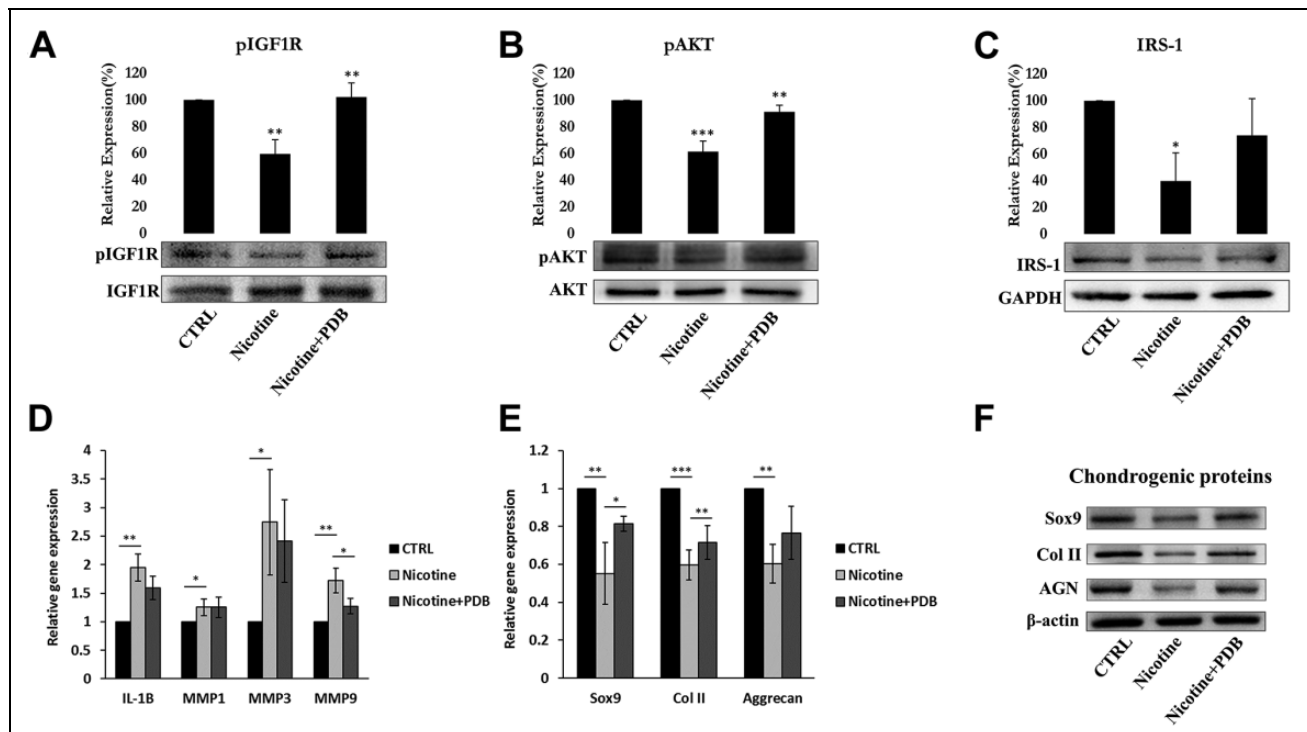


Figure 6. PDB regulated IGF-1 signaling, inflammatory profile and chondrogenesis in IVD. Protein levels of (A) pIGF-1 and (B) pAKT and (C) IRS-1 in control, nicotine-treated and PDB-treated nicotine-IVD group. (D) Gene expression of inflammatory molecules, including IL-1 β , MMP-1, MMP-3, and MMP-9. (E) Gene and (F) protein levels of chondrogenic markers (SOX9, Col II and aggrecan). The results are presented as mean \pm S.D. ($n = 3$; * $P < 0.05$, ** $P < 0.01$, *** $P < 0.001$).

had implicated beneficial effect of IGF-1 in producing ECM in human endplate chondrocytes³⁰. Further IGF-1/IRS pathway could modulate the phosphorylation of PI3K/AKT, thereby regulate the synthesis of ECM proteins during chondrocyte early development³¹. Our results clearly showed that nicotine inhibited the protein levels of IGF-1 signaling pathway, in particular pIGF-1 R (Fig. 6A), pAKT (Fig. 6B), and IRS-1 (Fig. 6C) in IVD compared to control. However, PDB significantly upregulated these levels implying a positive regulator of IGF-1 signaling pathway leading to increased ECM biosynthesis.

PDB Retarded Inflammatory Biomarkers profile in Nicotine-Induced IVD degeneration

The PI3K/AKT signaling is known to trigger the production of matrix metalloproteinases (MMPs), which are the inflammatory biomarkers responsible for degradation of cartilaginous extracellular matrix³². Hence, we attempted to determine catabolic MMPs such as IL-1 β , MMP-1, MMP-3, and MMP-9 in cartilaginous matrix of nicotine-induced IVD. The qPCR analysis exhibited increased levels of these inflammatory biomarkers in nicotine-treated groups as compared to controls (Fig. 6D). However, all the inflammatory molecules were suppressed in the PDB-treated group, indicating its anti-inflammatory characteristics.

Impact of PDB on Chondrogenic Markers in Nicotine-Induced IVD Degeneration

In the line with in vitro data, the levels of chondrocyte-lineage-specific genes (Fig. 6E) and proteins (Fig. 6F) including SOX9, Col II, and AGN were highly reduced in nicotine-treated group. However, PDB therapy restored these chondrogenic biomarkers. These data suggest that nicotine adversely influence IVD leading to degeneration of chondrocytes, which could be evidenced through loss of collagen and PG, yet could be repaired and regenerated by PDB treatment.

Discussion

In this study, we have presented the evidences of PDB therapeutic efficacy on nicotine-induced IVD degeneration. Through applying the increasing doses of nicotine to mimic the accumulation, the ihNPs population was significantly reduced. Further, pathophysiologic characteristics were revealed at molecular level in the terms of inhibited levels of chondrogenic-specific genes and proteins respectively, including SOX9, Col II and AGN, which were also confirmed through the feeble alcian blue staining in nicotine treated group, implying decreased proteoglycan (PG) content, hence a suppressed chondrogenesis. The pathophysiologic impacts of nicotine may be attributed to different

stereoisomeric forms of nicotine; in particular the (-)-nicotine which is comparatively highly active and greater toxic than (+)-nicotine³³. Compared to control, the inhibited proliferation and reduced mRNA levels of Sox9, type II collagen and aggrecan in nicotine-treated group is supported by previous reports^{34,35}, which indicate nicotine toxicity on IVD, resulting into degenerative phenotype. Similar to our study, nicotine adversely influenced the proliferation and chondrogenic differentiation of mesenchymal stem cells from the human Wharton's jelly, and this impairment was indicated through mediation of $\alpha 7$ nicotinic acetylcholine receptors³⁶.

After corroborating nicotine-induced IVD degeneration, we employed platelet-derived biomaterials (PDB), a concentrated platelet releasate, exerting various therapeutic applications due to their strong anti-inflammatory, reparative and regenerative activities^{16,37}. In this study, the reduced chondrogenic proteins and PG content in nicotine induced-IVD group was enhanced by PDB therapy, indicating its retardant effects to nicotine-mediated degenerative IVD. It is notable that nicotine is a cholinergic alkaloids, and depending on ingested dose, it could bind to central and peripheral nicotinic and muscarinic receptors, and finally modulate central nervous system, sympathetic autonomic, parasympathetic autonomic, and exert neuromuscular effects in varying combinations³⁸. Nicotine-mediated activities have been proposed to act into two phases, that is, stimulatory and later the inhibitory one. Firstly, nicotine act as an agonist at nicotinic receptor leading to a stimulatory effect on sympathetic system, which later blocks the receptor directing blockade of late parasympathetic and neuromuscular effects. Hence the pathological influence of nicotine on degenerative IVD phenotype during our *in vivo* and *in vitro* studies could be ascribed to preponderance of inhibitory response of chronic accumulation of nicotine. In our previous report, we have already demonstrated the use of higher doses of nicotine to mimic chronic accumulation in an osteoarthritis mice model¹⁴. Besides, previous study by Na An et al. employed a high range of doses of nicotine (10 μ M-10 mM) and found its detrimental impact on functions of human umbilical vein endothelial cells (HUVECs)¹⁵, playing a key role in progression of both cardiovascular disease and periodontal disease. This study specifically revealed that it is not the lower dose (10 μ M), but higher dose (10 mM) of nicotine inhibited HUVECs, indicating the chronic accumulation-mimicking ability of nicotine. Since nicotine could be uptaken transdermally through skin in daily life, we established nicotine-induced IVD degeneration mice model through subcutaneous injection.

The therapeutic effect of PDB in nicotine-induced IVD degeneration could be attributed to released growth factors, like insulin-like growth factor-1 (IGF-1), vascular endothelial growth factor (VEGF), hepatocyte growth factor (HGF), epidermal growth factor (EGF), adenosine triphosphate (ATP) and adenosine diphosphate (ADP)³⁹. We have previously showed that three-dimensional cultures are crucial for

normal chondrocyte physiology in tissue-engineered constructs, which mimic its *in vivo* microenvironment⁴⁰. Our results revealed that nicotine treatment altered the neo-cartilage morphology and suppressed the synthesis of ECM. However, after PDB treatment, the enhanced Col II and alcian blue stains indicated a restored gelatinous chondrogenic ECM in nucleus pulposus, and hence the chondrocytes recovery. Further, since creation of animal model plays a crucial role in understanding degenerative human IVD pathophysiology, we established nicotine-induced IVD degeneration mouse model, to investigate the *in vivo* effects of subcutaneously administered PDB, which revealed a prominent recovery from deformed nucleus pulposus, and proteoglycans in nicotine-treated group, leading to increased disc height index. These therapeutic efficacies of PDB might also be attributed to potent mitogenic and antifibrotic activities of HGF in nucleus pulposus⁴¹, regulating repair of inflamed tissues leading to matrix restoration⁴². Though intradiscally injected potential cell therapies have been commonly reported, to our knowledge, this is the first evidence of subcutaneously injected therapy in mouse model of IVD degeneration. A few similar studies were conducted by using MSCs; however, the cells either did not persist or generated unstable cartilage *in vivo*⁴³. Other report revealed that the injected region turned into vascularized and calcified⁴⁴.

It has already further been established that IGF-1/AKT regulatory machinery may control the development of IVD, by regulating proteoglycan synthesis in healthy chondrocytes^{45,46}. We evidenced that phosphorylated level of IGF-1, AKT, and IRS-1 was significantly declined in nicotine-treated group, and was later restored by PDB. These results are also in line with the previous study showing nicotine exposure would inhibit IGF-1 signaling pathway, including IGF-1 R, IRS1, and AKT-1/2, which may directly cause the reduction of extracellular matrix (ECM) synthesis, leading to retarded chondrogenesis⁴⁷. It has also noted that PI3K/AKT signaling axis may stimulate the production of MMPs⁴⁸. MMPs are proteolytic enzymes and associated with degradation of the matrix components of the IVD. Basaran et al. reported that IVD degeneration was positively affected by increased expression of MMPs such as MMP-1, -2, -3, and -9⁴⁹. Our previous study on nicotine-induced osteoarthritis also exhibited an elevated expression of inflammatory biomarkers, including IL-1 β , MMP-1, MMP-3, and MMP-9, which were further significantly decreased in PDB-treated groups¹⁴.

Additionally, according to previous studies, the accumulation of nicotine would induce hypertrophy of vascular walls, causing the narrowing of vascular network surrounding IVD, thereafter limit the exchange of anabolic agents and nutrients from blood to disc, this would eventually decrease the synthesis of proteoglycan and collagen, afterwards facilitate the IVD degeneration⁵⁰⁻⁵². Meanwhile, many studies indicated that the abundant growth factors of PDB could promote neovascularization⁵³⁻⁵⁵, in which may help disc cells to access nutrients and anabolic agents from blood,

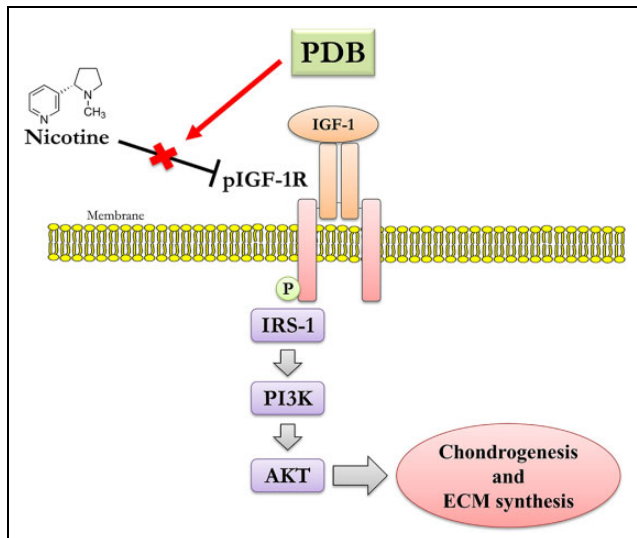


Figure 7. Possible mechanistic insight of therapeutic PDB in nicotine-induced IVD degeneration.

further recover the degeneration of IVD. Moreover, subcutaneous injection of PRP had been indicated increasing cartilage viability through enhancing the vascularity of the periphery vessels⁵⁶. Hence, except for the above-mentioned mechanism, the therapeutic effects of subcutaneous PDB in this study may also achieved possibly through improving the vascular network surrounding IVD. However, the detailed mechanism remains to be investigated in further researches.

Conclusively, PDB performed as an efficient therapeutic to IVD degeneration, through restoring the nicotine-inhibited IGF-1 signaling pathway, including the expression of pIGF-1 R, pAKT, and IRS-1, assisting the recovery of ECM synthesis and chondrogenesis (Fig. 7). Also, through suppressing the nicotine-induced inflammatory markers in IVD, PDB could engender the elevated levels of cartilage-specific genes and proteins (SOX9, Col II and aggrecan), hence promoting the regenerative effects on IVD degeneration.

Declaration of Conflicting Interests

The author(s) declared no potential conflicts of interest with respect to the research, authorship, and/or publication of this article.

Ethical Approval

All experimental protocols and animal care in this study were approved by the Institutional Animal Care and Use Committee (IACUC), Taipei Medical University Taiwan.

Statement of human and animal rights

All procedures in this study were conducted in accordance with the guidelines approved by the institutional review boards (IRB) of Taipei Medical University (IRB. No. 201305026).


Statement of Informed Consent

Written informed consent was obtained from the patients for their anonymized information to be published in this article.

Funding

The author(s) disclosed receipt of the following financial support for the research, authorship, and/or publication of this article: This work was supported by the following grants and agencies: Taiwan Ministry of Science and Technology [MOST 108-2221-E-038-014] and [MOST 110-2314-B-038-026], Taipei Medical University [TMU 108-5601-004-111] and Stem Cell Research Center, College of Oral Medicine, Taipei Medical University, Taiwan.

ORCID iD

Win-Ping Deng  <https://orcid.org/0000-0003-2180-0472>

References

1. Zhao C-Q, Jiang L-S, Dai L-Y. Programmed cell death in intervertebral disc degeneration. *Apoptosis*. 2006;11(12):2079–2088.
2. Zhao C-Q, Wang L-M, Jiang L-S, Dai L-Y. The cell biology of intervertebral disc aging and degeneration. *Ageing Res Rev*. 2007;6(3):247–261.
3. Trout JJ, Buckwalter JA, Moore KC, Landas SK. Ultrastructure of the human intervertebral disc. I. changes in notochordal cells with age. *Tissue Cell*. 1982;14(2):359–369.
4. An HS, Masuda K, Inoue N. Intervertebral disc degeneration: biological and biomechanical factors. *J Orthop Sci*. 2006;11(5):541–552.
5. Dowdell J, Erwin M, Choma T, Vaccaro A, Iatridis J, Cho SK. Intervertebral disk degeneration and repair. *Neurosurgery*. 2017;80(3 S): S46–S54.
6. Jackson AR, Dhawale AA, Brown MD. Association between intervertebral disc degeneration and cigarette smoking: clinical and experimental findings. *J Bone Joint Surg*. 2015;3(3):e2.
7. Scott SC, Goldberg MS, Mayo NE, Stock SR, Poitras B. The association between cigarette smoking and back pain in adults. *Spine*. 1999;24(11):1090–1098.
8. Benowitz NL. Pharmacologic aspects of cigarette smoking and nicotine addiction. *N Engl J Med*. 1988;319(20):1318–1330.
9. Uematsu Y, Matuzaki H, Iwahashi M. Effects of nicotine on the intervertebral disc: an experimental study in rabbits. *J Orthop Sci*. 2001;6(2):177–182.
10. Ernst E. Smoking, a cause of back trouble? *Rheumatology*. 1993;32(3):239–242.
11. Ernst E. Smoking is a risk factor for spinal diseases. hypothesis of the pathomechanism. *Wien Klin Wochenschr*. 1992;104(20):626.
12. Akmal M, Kesani A, Anand B, Singh A, Wiseman M, Goodship A. Effect of nicotine on spinal disc cells: a cellular mechanism for disc degeneration. *Spine*. 2004;29(5):568–575.
13. Uei H, Matsuzaki H, Oda H, Nakajima S, Tokuhashi Y, Esumi M. Gene expression changes in an early stage of intervertebral disc degeneration induced by passive cigarette smoking. *Spine*. 2006;31(5):510–514.
14. Lo W-C, Dubey NK, Tsai F-C, Lu J-H, Peng B-Y, Chiang P-C, Singh AK, Wu C-Y, Cheng H-C, Deng W-P. Amelioration of nicotine-induced osteoarthritis by platelet-derived biomaterials through modulating IGF-1/AKT/IRS-1 signaling Axis. *Cell Transplant*. 2020;29:0963689720947348.

15. An N, Andrukhov O, Tang Y, Falkensammer F, Bantleon HP, Ouyang X, Rausch-Fan X. Effect of nicotine and porphyromonas gingivalis lipopolysaccharide on endothelial cells in vitro. *PLoS One*. 2014;9(5):e96942.
16. Yip HK, Chen KH, Dubey NK, Sun CK, Deng YH, Su CW, Lo WC, Cheng HC, Deng WP. Cerebro- and renoprotective activities through platelet-derived biomaterials against cerebrorenal syndrome in rat model. *Biomaterials*. 2019;214:119227.
17. Rustenburg CM, Emanuel KS, Peeters M, Lems WF, Vergroesen PPA, Smit TH. Osteoarthritis and intervertebral disc degeneration: quite different, quite similar. *JOR spine*. 2018;1(4):e1033.
18. Yunus MHM, Nordin A, Kamal H. Pathophysiological perspective of osteoarthritis. *Medicina*. 2020;56(11):614.
19. Urban JP, Roberts S. Degeneration of the intervertebral disc. *Arthritis Res Ther*. 2003;5(3):1–11.
20. Wang Y, Wei L, Zeng L, He D, Wei X. Nutrition and degeneration of articular cartilage. *Knee Surg Sports Traumatol Arthrosc*. 2013;21(8):1751–1762.
21. Zhu Q, Jackson AR, Gu WY. Cell viability in intervertebral disc under various nutritional and dynamic loading conditions: 3d finite element analysis. *Journal of biomechanics*. 2012;45(16):2769–2777.
22. Kiyono T, Foster SA, Koop JJ, McDougall JK, Galloway DA, Klingelhutz AJ. Both Rb/p16 INK4a inactivation and telomerase activity are required to immortalize human epithelial cells. *Nature*. 1998;396(6706):84–88.
23. Hung SC, Yang DM, Chang CF, Lin RJ, Wang JS, Tone Ho L, Yang WK. Immortalization without neoplastic transformation of human mesenchymal stem cells by transduction with HPV16 E6/E7 genes. *Int J Cancer*. 2004;110(3):313–319.
24. Chen WH, Lo WC, Lee JJ, Su CH, Lin CT, Liu HY, Lin TW, Lin WC, Huang TY, Deng WP. Tissue-engineered intervertebral disc and chondrogenesis using human nucleus pulposus regulated through TGF- β 1 in platelet-rich plasma. *J Cell Physiol*. 2006;209(3):744–754.
25. Wei H-J, Wu AT, Hsu C-H, Lin Y-P, Cheng W-F, Su C-H, Chiu W-T, Whang-Peng J, Douglas FL, Deng W-P. The development of a novel cancer immunotherapeutic platform using tumor-targeting mesenchymal stem cells and a protein vaccine. *Mol Ther*. 2011;19(12):2249–2257.
26. Wu C-C, Chen W-H, Zao B, Lai P-L, Lin T-C, Lo H-Y, Shieh Y-H, Wu C-H, Deng W-P. Regenerative potentials of platelet-rich plasma enhanced by collagen in retrieving pro-inflammatory cytokine-inhibited chondrogenesis. *Biomaterials*. 2011;32(25):5847–5854.
27. Mangubat M, Lutfy K, Lee ML, Pulido L, Stout D, Davis R, Shin C-S, Shahbazian M, Seasholtz S, Sinha-Hikim A. Effect of nicotine on body composition in mice. *J Endocrinol*. 2012;212(3):317–326.
28. Chen W-H, Liu H-Y, Lo W-C, Wu S-C, Chi C-H, Chang H-Y, Hsiao S-H, Wu C-H, Chiu W-T, Chen B-J. Intervertebral disc regeneration in an ex vivo culture system using mesenchymal stem cells and platelet-rich plasma. *Biomaterials*. 2009;30(29):5523–5533.
29. Pockert AJ, Richardson SM, Le Maitre CL, Lyon M, Deakin JA, Buttle DJ, Freemont AJ, Hoyland JA. Modified expression of the ADAMTS enzymes and tissue inhibitor of metalloproteinases 3 during human intervertebral disc degeneration. *Arthritis Rheum*. 2009;60(2):482–491.
30. Zhang T, Wang L, Fang B, Wang H, Lu L. IGF-1 increases production of extracellular matrix in human endplate chondrocytes via distinct signaling pathways. *Int J Clin Exp Med*. 2019;12(7):8831–8838.
31. Starkman BG, Cravero JD, DelCarlo M Jr, Loeser RF. IGF-I stimulation of proteoglycan synthesis by chondrocytes requires activation of the PI 3-kinase pathway but not ERK MAPK. *Biochem J*. 2005;389(3):723–729.
32. Jiang R-H, Xu J-J, Zhu D-C, Li J-F, Zhang C-X, Lin N, Gao W-Y. Glycyrrhizin inhibits osteoarthritis development through suppressing the PI3K/AKT/NF- κ B signaling pathway in vivo and in vitro. *Food Funct*. 2020;11(3):2126–2136.
33. Barlow RB, Hamilton JT. The stereospecificity of nicotine. *Br J Pharmacol Chemother*. 1965;25(1):206–212.
34. Sive JI, Baird P, Jeziorski M, Watkins A, Hoyland JA, Freemont AJ. Expression of chondrocyte markers by cells of normal and degenerate intervertebral discs. *Mol Pathol*. 2002;55(2):91–97.
35. Park JY, Kuh SU, Park HS, Kim KS. Comparative expression of matrix-associated genes and inflammatory cytokines-associated genes according to disc degeneration: analysis of living human nucleus pulposus. *J Spinal Disord Tech*. 2011;24(6):352–357.
36. Yang X, Qi Y, Avercenc-Leger L, Vincourt JB, Hupont S, Huselstein C, Wang H, Chen L, Magdalou J. Effect of nicotine on the proliferation and chondrogenic differentiation of the human Wharton's jelly mesenchymal stem cells. *Biomed Mater Eng*. 2017;28(s1):S217–S228.
37. Chen WH, Lin CM, Huang CF, Hsu WC, Lee CH, Ou KL, Dubey NK, Deng WP. Functional recovery in osteoarthritic chondrocytes through hyaluronic acid and platelet-rich plasma-inhibited infrapatellar fat pad adipocytes. *Am J Sports Med*. 2016;44(10):2696–2705.
38. Davies P, Levy S, Pahari A, Martinez D. Acute nicotine poisoning associated with a traditional remedy for eczema. *Arch Dis Child*. 2001;85(6):500–502.
39. Murata S, Maruyama T, Nowatari T, Takahashi K, Ohkohchi N. Signal transduction of platelet-induced liver regeneration and decrease of liver fibrosis. *Int J Mol Sci*. 2014;15(4):5412–5425.
40. Chen WH, Lo WC, Hsu WC, Wei HJ, Liu HY, Lee CH, Tina Chen SY, Shieh YH, Williams DF, Deng WP. Synergistic anabolic actions of hyaluronic acid and platelet-rich plasma on cartilage regeneration in osteoarthritis therapy. *Biomaterials*. 2014;35(36):9599–9607.
41. Zou F, Jiang J, Lu F, Ma X, Xia X, Wang L, Wang H. Efficacy of intradiscal hepatocyte growth factor injection for the treatment of intervertebral disc degeneration. *Mol Med Rep*. 2013;8(1):118–122.
42. Sundman EA, Cole BJ, Karas V, Della Valle C, Tetreault MW, Mohammed HO, Fortier LA. The anti-inflammatory and

- matrix restorative mechanisms of platelet-rich plasma in osteoarthritis. *Am J Sports Med.* 2014;42(1):35–41.
43. De Bari C, Dell'Accio F, Luyten FP. Failure of in vitro-differentiated mesenchymal stem cells from the synovial membrane to form ectopic stable cartilage in vivo. *Arthritis Rheum.* 2004;50(1):142–150.
44. Peltari K, Winter A, Steck E, Goetzke K, Hennig T, Ochs BG, Aigner T, Richter W. Premature induction of hypertrophy during in vitro chondrogenesis of human mesenchymal stem cells correlates with calcification and vascular invasion after ectopic transplantation in SCID mice. *Arthritis Rheum.* 2006;54(10):3254–3266.
45. Loeser RF, Gandhi U, Long DL, Yin W, Chubinskaya S. Aging and oxidative stress reduce the response of human articular chondrocytes to insulin-like growth factor 1 and osteogenic protein 1. *Arthritis Rheumatol.* 2014;66(8):2201–2209.
46. Liu Z, Zhou K, Fu W, Zhang H. Insulin-Like growth factor 1 activates PI3k/Akt signaling to antagonize lumbar disc degeneration. *Cell Physiol Biochem.* 2015;37(1):225–232.
47. Deng Y, Cao H, Cu F, Xu D, Lei Y, Tan Y, Magdalou J, Wang H, Chen L. Nicotine-induced retardation of chondrogenesis through down-regulation of IGF-1 signaling pathway to inhibit matrix synthesis of growth plate chondrocytes in fetal rats. *Toxicol Appl Pharmacol.* 2013;269(1):25–33.
48. Greene MA, Loeser RF. Function of the chondrocyte PI-3 kinase-Akt signaling pathway is stimulus dependent. *Osteoarthritis Cartilage.* 2015;23(6):949–956.
49. Basaran R, Senol M, Ozkanli S, Efendioglu M, Kaner T. Correlation of matrix metalloproteinase (MMP)-1, -2, -3, and -9 expressions with demographic and radiological features in primary lumbar intervertebral disc disease. *J Clin Neurosci.* 2017;41:46–49.
50. Iwahashi M, Matsuzaki H, Tokuhashi Y, Wakabayashi K, Uematsu Y. Mechanism of intervertebral disc degeneration caused by nicotine in rabbits to explicate intervertebral disc disorders caused by smoking. *Spine.* 2002;27(13):1396–1401.
51. Elmasry S, Asfour S, de Rivero Vaccari JP, Travascio F. Effects of tobacco smoking on the degeneration of the intervertebral disc: a finite element study. *PLoS One.* 2015;10(8):e0136137.
52. Vo N, Wang D, Sowa G, Witt W, Ngo K, Coelho P, Bedison R, Byer B, Studer R, Lee J. Differential effects of nicotine and tobacco smoke condensate on human annulus fibrosus cell metabolism. *J Orthop Res.* 2011;29(10):1585–1591.
53. Zhang X, Shi K, Jia P, Jiang L, Liu Y, Chen X, Zhou Z, Li Y, Wang L. Effects of platelet-rich plasma on angiogenesis and osteogenesis-associated factors in rabbits with avascular necrosis of the femoral head. *Eur Rev Med Pharmacol Sci.* 2018;22(7):2143–2152.
54. Bir SC, Esaki J, Marui A, Yamahara K, Tsubota H, Ikeda T, Sakata R. Angiogenic properties of sustained release platelet-rich plasma: characterization in-vitro and in the ischemic hind limb of the mouse. *J Vasc Surg.* 2009;50(4):870–879. e2.
55. Cheng H, Zhang J, Li J, Jia M, Wang Y, Shen H. Platelet-rich plasma stimulates angiogenesis in mice which may promote hair growth. *Eur J Med Res.* 2017;22(1):1–6.
56. Bulam H, Ayhan S, Yilmaz G, Sezgin B, Sibar S, Tuncer S, Findikcioglu K, Latifoglu O. The effect of subcutaneous platelet-rich plasma injection on viability of auricular cartilage grafts. *J Craniofac Surg.* 2015;26(5):1495–1499.